ELSEVIER

Journal of Organometallic Chemistry 643–644 (2002) 441–452

Journal of Organometallic Chemistry

www.elsevier.com/locate/jorganchem

Stereomutation and apicophilicity of diastereomeric spirophosphoranes (10-P-5)

Masaaki Nakamoto, Satoshi Kojima, Shiro Matsukawa, Yohsuke Yamamoto, Kin-ya Akiba *

Department of Chemistry, Graduate School of Science, Hiroshima University, 1-3-1 Kagamiyama, Higashi-Hiroshima 739-8526, Japan

Received 27 July 2001; accepted 14 November 2001

Abstract

The apicophilicity for a series of monodentate groups were determined by deducing activation parameters of equilibration between diastereomeric spirophosphoranes bearing a Martin ligand and a modified Martin ligand. The equilibration was shown to be an intramolecular process and the order of apicophilicity of the groups turned out to be OMe ≈ H > COMe ≈ SMe > NMe_2 > Me > *n*-Bu on the basis of activation enthalpy. The involvement of π-conjugation type interactions was revealed by X-ray structures of symmetric analogs bearing COMe (acceptor) and NMe_2 (donor) groups. © 2002 Published by Elsevier Science B.V.

Keywords: Spirophosphorane; Pentacoordinate; Apicophilicity; Hypervalent; NMR; X-ray analysis

1. Introduction

Indications that pentacoordinate phosphorus intermediates are involved in biological transformations involving the phosphoryl group have stimulated studies on model phosphorane compounds [1,2]. In order to understand the mechanism of reactions involving these hypervalent species, there are two aspects that must be considered, which are characteristic of pentacoordinate compounds in general and are not very familiar in the chemistry of first row elements. They are pseudorotation, a kinetic aspect [3], and apicophilicity, a thermodynamic aspect [4]. The barrier of pseudorotation is usually relatively low, causing rapid stereomutations in contrast to tetracoordinate phosphorus species, which are ordinarily stereochemically rigid [2,5]. As for apicophilicity, the relative preference for substituents to occupy the apical positions as opposed to the equatorial positions in trigonal bipyramidal (TBP) structures, a number of experimental results [2,6] and theoretical calculations [7] have indicated that multiple factors are influential. A general propensity deduced from these results is that electronegative substituents prefer the apical positions, while π donative or bulky ligands prefer the equatorial positions. However, discrepancies between series of apicophilicity provided by several groups (deduced by different methods) have frequently been pointed out, among the experimental ones in particular. One of the reasons for this comes from the fact that the experimental apicophilicity scales have been established on the free energy of activation for pseudorotation of phosphoranes using dynamic NMR techniques, which is of kinetic and not of thermodynamic nature. Thus, when interconversion processes involve monocyclic and acyclic structures, what is actually being compared is the relative difference in energy between the most stable TBP ground state and the higher energy square pyramidal (SP) transition state along the reaction coordinate. According to definition, however, the ideal apicophilic scale should be deduced from the comparison of two isomeric TBP states in which the substituents in question can occupy an apical position in one state and an equatorial position in the other. Unfortunately, this ideal situation is attainable only in theoretical calculations, which allow the co-existence of such isomers which may differ greatly in energy, and in a very limited number of experimental exceptions [9d,9e]. Furthermore, concerning the stereoelectronic features of SP states, other than the

* Corresponding author. Present address: Advanced Research Center for Science and Engineering, Waseda University, 3-4-1 Ohkubo, Shinjuku-ku, Tokyo 169-8555, Japan. Tel./fax: +81-3-5286-3165.
E-mail address: akibaky@mn.waseda.ac.jp (K.-y. Akiba).

0022-328X/02/$ - see front matter © 2002 Published by Elsevier Science B.V.
PII: S0022-328X(01)01440-1

theoretical study by Schleyer and co-workers [7d], there are no reliable studies that actually link apicophilicity (by definition) and the pseudorotation barrier. In their analysis, it is shown that even for a simple one-step pseudorotation process, a complete linear correlation is not seen between the two. For spirophosphoranes with small ring sizes (five membered or less), there have been indications that the overall transition state (the transition state for the rate-determining pseudorotation process) involves either a TBP configuration in which one of the bidentates spans between two of the equatorial positions or an SP configuration close to this TBP, and that the energy surface in the vicinity of this configuration is rather flat [2]. This implies that although the true transition state might not be of TBP geometry, it will be very close to a TBP in terms of energy. Thus a spirophosphorane bearing two five-membered rings and a monodentate ligand can be used as a suitable model to determine apicophilicity of the monodentate ligand because the ground state is TBP and the transition state can also be regarded as TBP in which only the equatorial monodentate atom and a bidentate five-membered ring atom have changed places. Although such spirophosphoranes bearing five-membered rings have been examined for pseudorotation in the past, they were only a small set of compounds [6a,6b]. Furthermore, for this class of compounds, the analysis of activation enthalpy, which is a more universal parameter than the temperature-dependent activation free energy, has been overlooked. We have undertaken a systematic examination of apicophilicity using spirophosphoranes bearing monodentate substituents with a wide range of electronegativities by utilizing modified Martin spirophosphoranes [8,9], in which one of the trifluoromethyl groups has been replaced with a methyl group (**1**, **4**–**9**) [10]. Herein we describe our results [11].

2. Results and discussion

2.1. Synthesis and determination of stereochemistry

The preparation of 1-substituted spirophosphoranes is outlined in Scheme 1. 1-Hydrospirophosphorane **1** was prepared in 60% yield with a diastereomeric ratio of **1-exo**:**1-endo** as ca. 2:1 by the successive treatment of diethylaminodichlorophosphine with lithium 1,1,1,3,3,3-hexafluoro-2-(2-lithiophenyl)-2-propoxide (Martin ligand) followed by lithium 1,1,1-trifluoro-2-(2-lithiophenyl)-2-propoxide (modified Martin ligand; from 2-(2-bromophenyl)-1,1,1-trifluoro-2-propanol) and then acid. The deactivated phosphine, diethylaminodichlorophosphine, was required to control the successive introduction of the two ligands. The diastereomeric mixture could be readily separated by chromatography (silica gel, hexane/ether = 5/1), and each diastereomer was obtained as a crystalline solid stable to water.

1-Hydrospirophosphorane **1** was treated with several electrophiles (acetyl chloride, elemental sulfur then methyl iodide, methyl iodide and *n*-butyl bromide) in the presence of base (DBU or NaH) to afford 1-substituted spirophosphoranes in good yields via phosphoranide **2**. The electrophilic reaction proceeded with essentially full retention of configuration [10]. Other 1-substituted spirophosphoranes with electronegative groups (X = OMe, NMe_2) were obtained by nucleophilic substitutions of MeOH and Me_2NH on 1-chlorospirophosphorane **3**, which was generated from phosphoranide **2** with SO_2Cl_2. Using single diastereomers of **1-exo**, the resulting spirophosphoranes were obtained as diastereomeric mixtures in the case of **4** and **7**. This is probably due to the rapid stereomutation of 1-chlorospirophosphorane **3**. Phosphoranide **2** and 1-chlorospirophosphorane **3** were also found to be sensitive to moisture. Spirophosphoranes **4**–**9** were stable to moisture and heat. Owing to their relatively rigid stereochemistry, the diastereomeric pairs could be separated by chromatography, except for X = Me in which the pair had identical R_f values.

The relative stereochemistries of the spirophosphoranes were assigned by difference ^{1}H-NMR NOE experiments. The series of diastereomers in which irradiation of the bidentate CH_3 resulted in intensity enhancement at the monodentate bound to phosphorus and the *ortho* proton of the same bidentate could be assigned to the configuration designated **exo**, while the diastereomers in which irradiation of the bidentate CH_3 resulted in intensity enhancement at the two protons *ortho* to phosphorus in the bidentate ligands were designated **endo**. Thus the relative stereochemistries could be assigned as shown in Fig. 1.

X-ray analysis of **1-exo** verified our assignment of relative stereochemistry and showed nearly ideal TBP structure as expected (Fig. 2). The hydrogen atom attached to phosphorus was located on the difference Fourier map and was found to occupy one of the equatorial positions. It comes into notice that the more electron-withdrawing group elongates the apical bond (P–O(1) = 1.766 Å) compared to the other one (P–O(2) = 1.709 Å). The methyl group was found to be facing in the direction of the proton attached to phosphorus.

Stereomutation between the diastereomeric pairs occurred without any accompanying decomposition upon heating them in solution. In principle, no change in the chemical shifts or the shape of signals could be observed in NMR spectra upon changing solvents or temperature. This implies that the characteristic pentacoordinate TBP structures were maintained for all the compounds in solution.

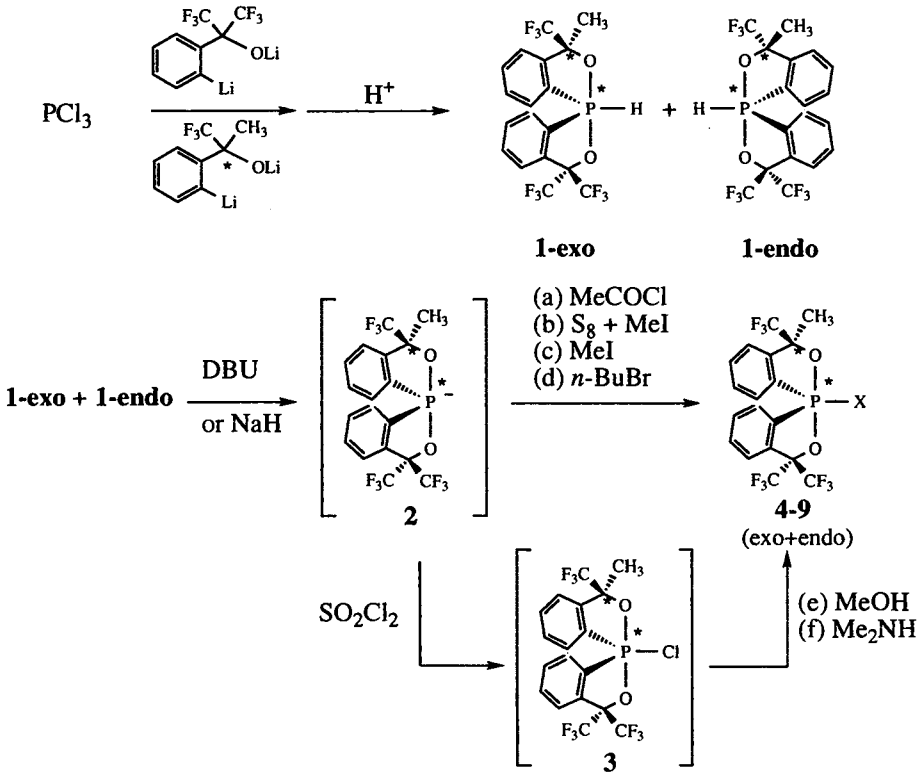

	X	Method	Yield	^{31}P NMR (δ, CDCl 3)		Diastereomeric ratio at equilibrium
			(%)	exo	endo	exo:endo
1	H	–	57	-49.4	-47.8	40:60 (40°C)
4	OMe	(e)	44	-16.3	-18.1	67:33 (40°C)
5	COMe	(a)	58	-37.1	-39.1	59:41 (90°C)
6	SMe	(b)	86	-24.1	-24.8	77:23 (80°C)
7	NMe_2	(f)	47	-29.5	-28.3	38:62 (150°C)
8	Me	(c)	62	-26.9	-26.1	50:50 (150°C)
9	*n*-Bu	(d)	63	-22.2	-22.7	56:44 (170°C)

Scheme 1.

2.2. Kinetic measurements

The equilibration processes of the diastereomers were monitored by ^{19}F-NMR signals of the pair of compounds (Scheme 2). The measurements were performed in aromatic hydrocarbons (toluene, *p*-xylene or *t*-butyltoluene) as solvent. In addition, pyridine was also used as solvent in order to investigate solvent effects in the case of X = OMe (**4**) and H (**1**). The former corresponds to the most polar phosphorane, and was thought most likely to be affected by donor solvents if there were any affect at all. As for the latter, P–H phosphoranes are generally known to be in equilibrium with ring opened tautomers, and thus stereomutation had the possibility to proceed via tautomeric phosphinites and base is expected to assist such tautomerization. The interconversion followed exact first-order kinetics and differences in concentrations (0.02–0.1 M)

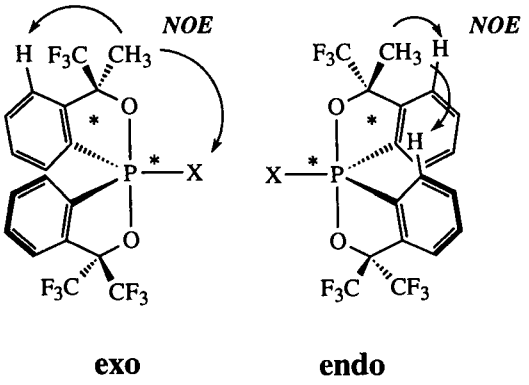

Fig. 1. Determination of relative stereochemistry by NOE measurements.

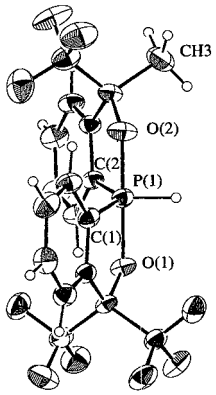

Fig. 2. ORTEP drawing of **1-exo** (X = H) with thermal ellipsoids at 30% probability level.

had no effect on the rate constants for all the phosphoranes examined. The activation parameters of the process were estimated from the Eyring plot of the rates for at least four different temperatures (Fig. 3 and Table 1).

In the case of **1**, there was practically no difference in the values of the activation parameters and the activation entropy was small regardless of the solvent used. If dissociation and/or association were the rate-determining step, a change in the reaction profile would have been expected. This would result in changes in the

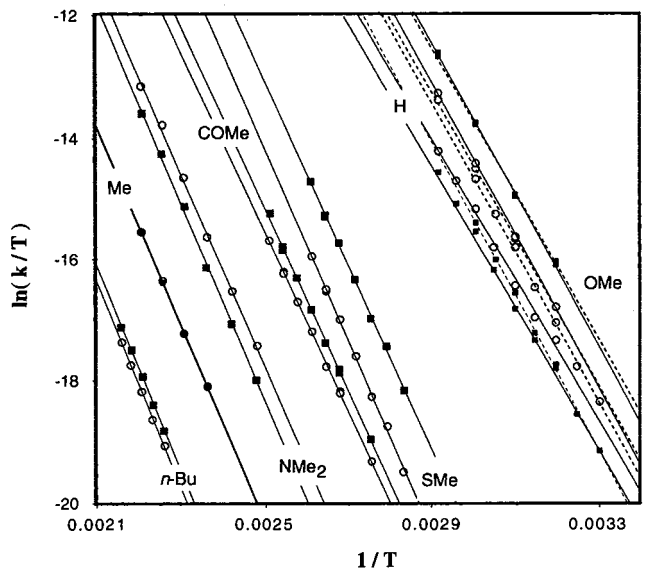

Fig. 3. Eyring plots of $1/T$ vs. $\ln(k/T)$ for the stereomutation of the diastereomers. Open circles correspond to the endo to exo process and filled squares to the exo to endo process. Solid lines are for measurements in aromatic hydrocarbon, whereas dashed lines are for those in pyridine.

activation parameters, especially in the entropy value, since transient zwitterionic phosphonium ions would be involved. Thus, the stereomutation process involving P–O bond dissociation–recombination is unlikely. Other experimental facts were supportive of this interpretation. Less than 5% deuteration of **1-exo** could be observed upon dissolution of this compound in CD_3OD even after the elapse of 24 h. During this time, however, more than 10% had undergone stereomutation to **1-endo**. On the other hand, upon addition of four equivalents of pyridine to the above solution, H–D exchange was complete within 30 min, without any apparent change in diastereomeric ratio [^{31}P-NMR in CD_3OD for **1-exo**-D: -50.1 ($J_{P-D} = 110$ Hz), for **1-endo**-D: -48.7 ($J_{P-D} = 107$ Hz)]. Furthermore, only a small isotope effect ($k_H/k_D = 1.1$) was observed for the stereomutation at 50 °C. These results clearly show that there is no relation between stereomutation and H–D exchange or P–O bond dissociation.

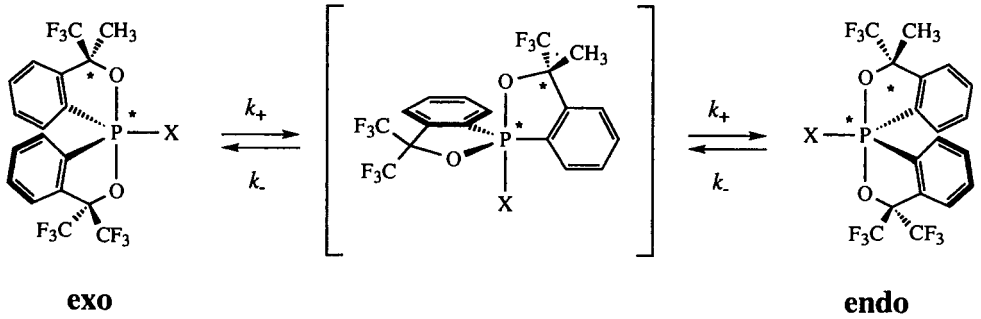

Scheme 2.

Table 1
Activation parameters for stereomutation of 1-substituted spirophosphoranes

X		Solvent	exo to endo			endo to exo		
			$\Delta H^{\ddagger}$ [a] (kcal mol^{-1})	$\Delta S^{\ddagger}$ [a] (eu)	$\Delta G^{\ddagger}_{298}$ (kcal mol^{-1})	$\Delta H^{\ddagger}$ [a] (kcal mol^{-1})	$\Delta S^{\ddagger}$ [a] (eu)	$\Delta G^{\ddagger}_{298}$ (kcal mol^{-1})
OMe	(**4**)	*p*-Xylene	24.2 ± 0.5	-3.3 ± 1.6	25.2	24.0 ± 0.5	-2.6 ± 1.6	24.7
		Pyridine	25.1 ± 0.6	0.3 ± 1.7	25.2	24.9 ± 0.6	-0.6 ± 1.7	24.8
H	(**1**)	Toluene	24.2 ± 0.5	-4.9 ± 1.4	25.6	24.4 ± 0.5	-5.0 ± 1.4	25.8
		Pyridine	24.4 ± 0.8	-3.1 ± 2.5	25.3	25.1 ± 0.7	-2.4 ± 2.3	25.8
COMe	(**5**)	*p*-Xylene	29.4 ± 0.3	-4.5 ± 0.9	30.8	30.0 ± 0.4	-2.3 ± 1.0	30.7
SMe	(**6**)	*p*-Xylene	30.8 ± 0.6	1.4 ± 1.5	30.3	29.9 ± 0.6	1.6 ± 1.7	29.4
NMe_2	(**7**)	4-Butyltoluene	31.8 ± 0.6	-3.0 ± 1.4	33.2	32.4 ± 0.6	-2.6 ± 1.4	32.7
Me	(**8**)	4-Butyltoluene	33.5 ± 0.6	-4.0 ± 1.3	34.7	33.5 ± 0.6	-4.0 ± 1.3	34.7
n-Bu	(**9**)	4-Butyltoluene	33.8 ± 0.9	-8.7 ± 1.9	36.4	33.5 ± 0.9	-8.8 ± 1.9	36.1

[a] Accuracy is shown as standard deviation.

For phosphorane **4**, activation parameters were similar in both *p*-xylene and pyridine just as for **1**. Thus, we can conclude that nucleophilic assistance seen for stiboranes [11b] is not involved here, and stereomutation is straightforward. For other phosphoranes, the values of activation entropy were near zero (less than five) except for X = *n*-Bu (**9**). These kinetic features indicate that the stereomutation of the whole series of compounds should be of intramolecular nature without bond dissociation which would gives rise to zwitterionic phosphonium ions. Thus, we arrive at an order of activation enthalpies of OMe ≈ H < COMe ≈ SMe < NMe_2 < Me ≈ *n*-Bu (see Table 1).

All stereomutation pathways of spirophosphoranes, **1**, **4**–**9**, by Berry pseudorotation can be topologically depicted by the diagram shown in Fig. 4 [12]. With our compounds, the ground state spirophosphoranes are 21 or 12 (the former is **exo** and the latter is **endo**). We can deduce from this diagram that all multi-step pseudorotation processes involve a high energy phosphorane with a diequatorial five-membered ring (species with index *n*5 or 5*n*, which are depicted with filled squares in Fig. 4). Among these configurations, 35, 53 and 45, 54 are expected to be least favorable since in addition to having ring strain resulting from the diequatorial bidentate, they have unfavorable carbon atoms of the bidentate in the apical position. Thus, these isomers can be counted out and the lowest possible energy pseudorotation pathways become those given in Scheme 3. For cyclic phosphoranes (five-membered ring), as stated above, high energy configurations such as 15, 51 and 25, 52 can be regarded as the transition state (or at least energetically close) [2,7e]. Therefore the value of $\Delta G^{\ddagger}$ for the pseudorotation between the ground state phosphoranes (equatorial monodentate) and the transition state (apical monodentate) could be regarded as directly related to the relative apicophilicity of the monodentate attached to the phosphorus. The relative apicophilicity scale can be deduced from the results given in Table 1. On the basis of the values of $\Delta H^{\ddagger}$ of these compounds, we can conclude that the relative apicophilicity of monodentate ligand is in the order of OMe ≈ H > COMe ≈ SMe > NMe_2 > Me ≈ *n*-Bu.

One can see that this apicophilicity scale does not follow the electronegativity scale (Table 2). This is most obvious for the COMe and NMe_2 groups. For the COMe group it should be noted that it is more apicophilic than alkyl groups (Me or Bu) by 4 kcal mol^{-1} and less apicophilic than the OMe group having similar electronegativity by 6 kcal mol^{-1}. Thus, we can see that the identity of the element directly attached to the phosphorus atom has a large contribution on apicophilicity. However, stabilization of the electron-rich apical bond by conjugation with C=O π* seems also to be of significance. This notion is supported by the X-ray structure of **5′** (Fig. 5), in which the Me of **5** has

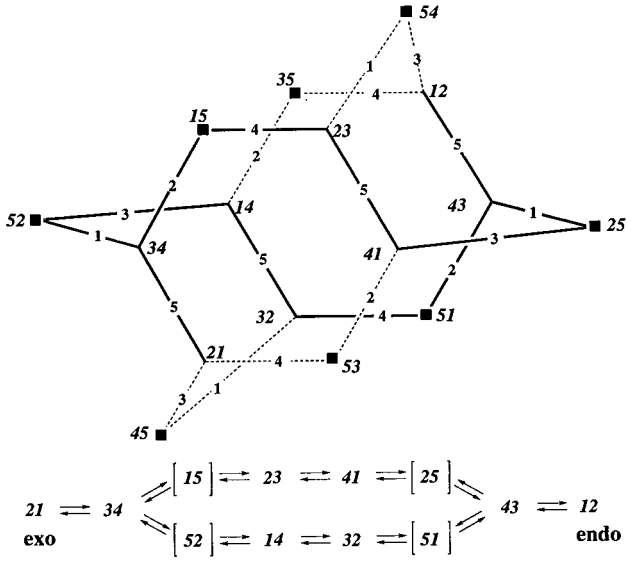

Fig. 4. Restricted Desargus–Levi diagram. The double digits correspond to diastereomers and the single digits to the pivot substituent of the pseudorotation process.

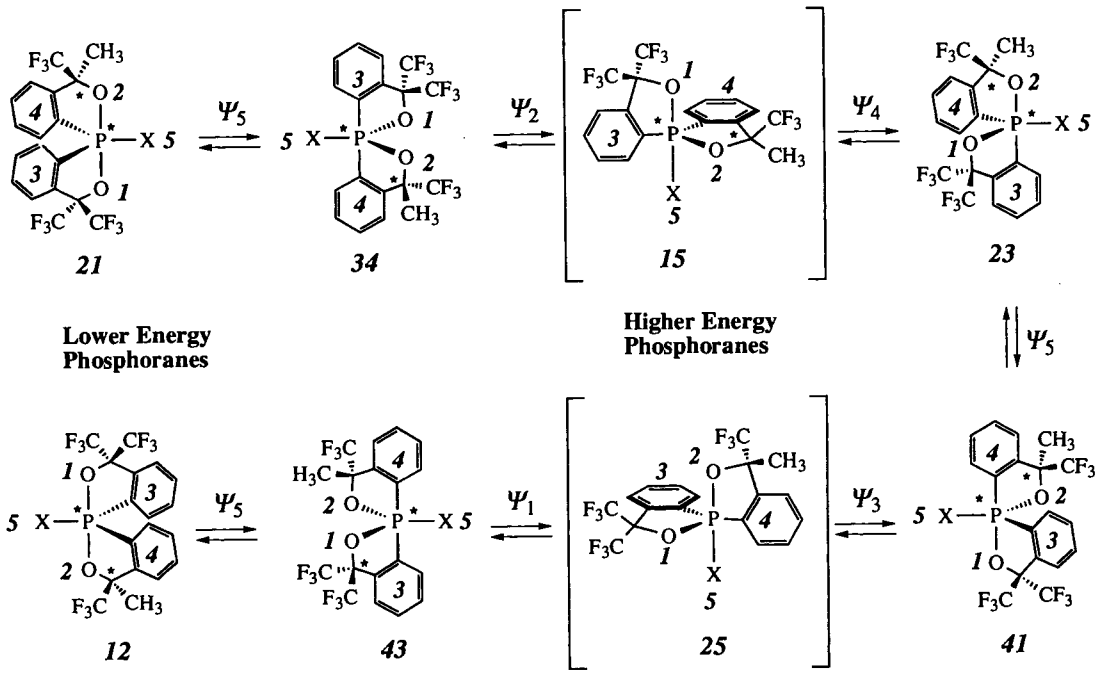

Scheme 3.

Table 2
Relative apicophilicity of monodentate ligands

Relative apicophilicity	OMe	≈	H	>	COMe	≈	SMe	>	NMe_2	>	Me	≈	*n*-Bu
$\Delta H^{\ddagger}$ [a]	24.1		24.3		29.7		30.0		32.1		33.5		33.7
Electronegativity [b]	2.68		(2.10)		2.69		2.45		2.40		2.27		(2.28)
Group electronegativity [c]	3.7		2.28		2.85		2.8		3.0		2.3		2.3
σ_1 [d]	0.3		0.0		0.3		0.3		0.17		−0.10		−0.10

[a] Average $\Delta H^{\ddagger}$ of the values of exo to endo and endo to exo.
[b] Ref. [13].
[c] Ref. [14].
[d] Ref. [15].

been replaced by a CF_3 group. As can be seen, the carbonyl group is practically coplanar with the atoms constituting the equatorial plane. Or in other words, the supposedly present π-orbitals of the carbonyl group are practically parallel with the apical bond. The possibility of such a phenomenon has been hinted at in theoretical calculations [7h].

The difference in apicophilicity between the OMe and NMe_2 groups is about 8 kcal mol^{-1}. This implies the presence of a large π-type interaction between the equatorial nitrogen lone pair and σ* orbitals of the two other equatorial P–C bonds, and is in good agreement with assumptions from theoretical calculations [7d]. X-ray analysis of **7′** (Fig. 6), the symmetric analog of **7** (CF_3 in the place of Me) is supportive in this case also. Thus, the nitrogen atom is practically flat (sp^2), and the N–C bonds are nearly coplanar with the apical bond (implying that the lone pair on nitrogen is essentially in the equatorial plane). Although OMe is also capable of

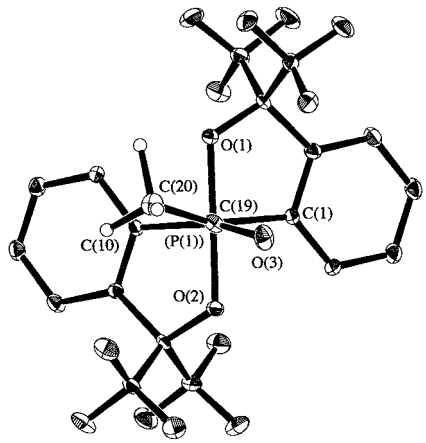

Fig. 5. ORTEP drawing of **5′** (X = COMe) viewed along the direction of the axis of the P–C(carbonyl) bond with thermal ellipsoids at 30% probability level. Hydrogen atoms other than for the acetyl group have been omitted for clarity.

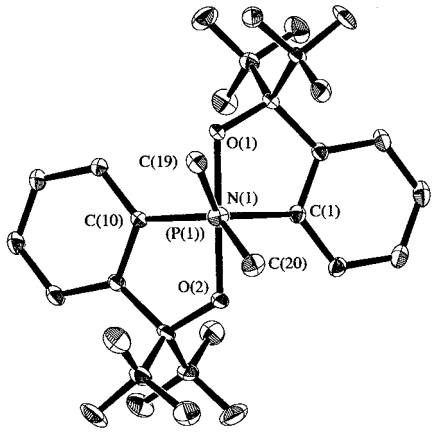

Fig. 6. ORTEP drawing of **7′** (X = NMe_2) viewed along the direction of the axis of the P–N bond with thermal ellipsoids at 30% probability level. Hydrogen atoms have been omitted for clarity.

such interactions, having lone pair electrons, because of the highly electronegative nature of the oxygen atom, this factor is expected to be of little significance. As for the effect of sterics in compounds **5′** and **7′**, since the P–N bond is shorter than the P–C(carbonyl) bond and a NMe_2 group is larger than a MeCO group, the former group is expected to be more susceptible to steric hindrance. For the remainder of the compound, the moieties exerting the largest steric hindrance towards the monodentate are the exo CF_3 groups. However, contrary to expectations from this sterical point of view, the more hindered NMe_2 compound has the methyl groups closer to the CF_3 groups. This observation supports the rationalization of the X-ray structures based upon electronic effects as mentioned above (Tables 3 and 4).

Hence, π-acceptor ligand COMe and π-donor ligand NMe_2 have higher equatorial site preference than expected from the electronegativity factor. Although a good correlation between inductive substituent constant σ_I and relative apicophilicity scales has been demonstrated by Cavell and Buono, etc. [6], the correlation is not strong in our case although activation enthalpy is considered. Thus, we can conclude that the element factor is of primary importance while π-type interactions also contribute largely to relative apicophilicity.

The large negative entropy value for **9** (X = *n*-Bu) compared with **8** (X = Me) can be accounted for by considering the fact that, generally, the apical position (which in this case should correspond to the transition

Table 3
Crystallographic data for **1**, **5′**, and **7′**

Compound	**1** (X = H)	**5′** (X = COMe)	**7′** (X = NMe_2)
Empirical formula	$C_{18}H_{11}F_9O_2P$	$C_{20}H_{11}F_{12}O_3P$	$C_{20}H_{14}F_{12}NO_2P$
Formula weight	462.25	558.26	559.29
Crystal system	Orthorhombic	Monoclinic	Orthorhombic
Space group	*Pbca*	*Cc*	*Pbca*
Crystal size (mm)	$0.50 \times 0.40 \times 0.40$	$0.50 \times 0.40 \times 0.20$	$0.55 \times 0.50 \times 0.30$
Color	Colorless	Colorless	Colorless
Habit	Prism	Plate	Prism
a (Å)	19.501(4)	16.7000(4)	7.5340(1)
b (Å)	20.759(5)	6.9890(2)	21.6040(6)
c (Å)	9.152(2)	17.9830(4)	26.7650(7)
α (°)	90	90	90
β (°)	90	102.456(2)	90
χ (°)	90	90	90
V (Å^3)	3704(1)	2049.50(9)	4356.4(2)
Z	8	4	8
Θ_{min}	12.4	12.6	12.6
Θ_{max}	27.5	28.0	27.9
D_{calc} (g cm^{-3})	1.657	1.809	1.705
Absorption coefficient (mm^{-1})	0.249	0.266	0.248
F(000)	1848	1112	2240
Radiation; λ (Å)	Mo–K_α, 0.7107	Mo–K_α, 0.7107	Mo–K_α, 0.7107
Temperature (K)	298	130	130
Data collected	$+h, \pm k, \pm l$	$+h, +k, \pm l$	$+h, +k, +l$
Total reflections collected	3942	2513	5582
Reflections unique	3413	2357	4962
Reflections used	3413	2357	4962
Number of parameters refined	271	325	325
R, R_w	0.0436, 0.1394	0.0429, 0.1287	0.0556, 0.2159
Goodness-of-fit (obs.)	1.028	1.019	1.033
Maximum shift in final cycle	0.0027	0.0006	0.0013
Final diff. map, max (e Å^{-3})	0.20	0.24	0.19

Table 4
Selected structural parameters for **1**, **5′**, and **7′**

	1 (X = H)		**5′** (X = COMe)		**7′** (X = NMe_2)
Bond lengths					
P(1)–O(1)	1.710(2)	P(1)–O(1)	1.761(2)	P(1)–O(1)	1.739(1)
P(1)–O(2)	1.765(2)	P(1)–O(2)	1.747(2)	P(1)–O(2)	1.740(1)
P(1)–C(1)	1.814(3)	P(1)–C(1)	1.805(3)	P(1)–C(1)	1.831(2)
P(1)–C(10)	1.810(3)	P(1)–C(10)	1.811(3)	P(1)–C(10)	1.832(2)
P(1)–H(12)	1.286(1)	P(1)–C(19)	1.870(3)	P(1)–N(1)	1.658(2)
Bond angles					
O(1)–P(1)–O(2)	179.8(1)	O(1)–P(1)–O(2)	178.06(10)	O(1)–P(1)–O(2)	172.39(6)
O(1)–P(1)–C(1)	89.0(1)	O(1)–P(1)–C(1)	88.25(10)	O(1)–P(1)–C(1)	87.57(7)
O(2)–P(1)–C(10)	87.5(1)	O(2)–P(1)–C(10)	88.2(1)	O(2)–P(1)–C(10)	87.29(6)
C(1)–P(1)–C(10)	128.7(1)	C(1)–P(1)–C(10)	127.2(1)	C(1)–P(1)–C(10)	129.80(6)
C(1)–P(1)–H(12)	117.5(1)	C(1)–P(1)–C(19)	114.0(1)	C(1)–P(1)–N(1)	115.03(7)
C(10)–P(1)–H(12)	113.8(1)	C(10)–P(1)–C(19)	118.7(1)	C(10)–P(1)–N(1)	115.15(7)
		P(1)–C(19)–C(20)	116.8(2)	P(1)–N(1)–C(19)	124.0(1)
		P(1)–C(19)–O(3)	118.2(2)	P(1)–N(1)–C(20)	122.4(1)
		O(3)–C(19)–C(20)	125.0(3)	C(19)–N(1)–C(20)	112.2(2)
Torsion angles					
		O(1)–P(1)–C(19)–C(20)	70.9(2)	C(19)–N(1)–P(1)–C(1)	110.5(1)
		O(1)–P(1)–C(19)–O(3)	−108.2(2)	C(19)–N(1)–P(1)–C(10)	−70.8(2)
		O(2)–P(1)–C(19)–C(20)	−107.9(2)	C(20)–N(1)–P(1)–C(1)	−54.8(2)
		O(2)–P(1)–C(19)–O(3)	73.0(2)	C(20)–N(1)–P(1)–C(10)	123.8(1)
		Average torsion angle [a]	17.8	Average torsion angle [a]	62.8

[a] Average torsion angle from the equatorial plane.

state) is more sterically demanding than the equatorial position, and thus requires higher order among the substituents. The fact that activation enthalpy is essentially the same for the two substituents indicates that the electronic influence of the two substituents to apicophilicity is practically the same, and thus the observed large difference in rates or free energies of activation can be attributed almost completely to the difference in relative sterical demands between the two. This comparison presents an example where the separation of free energy of activation into enthalpy and entropy terms is effective in deducing the relative steric and electronic contributions to apicophilicity.

3. Conclusion

In conclusion, through the determination of the pseudorotational barriers for spirophosphoranes configurationally stable at room temperature, we have established yet another new system of pseudorotation that we believe to be highly reflective of the *energy differences between pseudorotamers of TBP character*. Thus, apicophilicity derived from activation enthalpy is OMe ≈ H > COMe ≈ SMe > NMe_2 > Me ≈ *n*-Bu. Also found was the importance of π-conjugation factors of the COMe and NMe_2 groups, which was supported by X-ray structural analysis. In the case of the Me and *n*-Bu groups, the use of activation enthalpy revealed that the electronic contribution could be exaggerated in observed pseudorotation rates, hence steric factors should not be ignored.

4. Experimental

4.1. General methods

All reactions involving air-sensitive chemicals were carried out under N_2. Ether and THF were freshly distilled from sodium–benzophenone and all other solvents were distilled from calcium hydride under an inert atmosphere. Merck silica gel was used for column chromatography and Merck silica gel 60 GF_{254} for TLC. Melting points were measured with a Yanagimoto micro melting point apparatus and are uncorrected. ^{1}H-NMR (400 MHz), ^{19}F-NMR (376 MHz) and ^{31}P-NMR (162MHz) spectra were recorded on a JEOL EX-400 spectrometer. Chemical shifts (δ) are reported as parts per million downfield from internal Me_4Si for ^{1}H, from external trichlorofluoromethane for ^{19}F and from external 85% H_3PO_4 for ^{31}P. Elemental analysis was performed on a Perkin–Elmer 2400 CHN elemental analyzer.

4.2. 3-Methyl-3,3′,3′-tris(trifluoromethyl)-1λ^5-1,1′(3H,3′H)-spirobi(2,1-benzoxaphosphole) (**1**)

To a solution of 1,1,1,3,3,3-hexafluoro-2-phenyl-2-propanol (5.8 g, 24 mmol) in dry ether (20 ml) was

added *n*-BuLi in hexane (1.6 M, 32 ml, 51 mmol) at −78 °C under N_2, followed by tetramethylethylenediamine (TMEDA, 0.28 g, 2.4 mmol). The solution was then allowed to warm to room temperature (r.t.). After stirring for 10 h, the dilithio salt of the alcohol which had precipitated was dissolved with THF (20 ml) to give a clear solution. The solution was added dropwise via cannula to diethylaminodichlorophosphine (3.55 g, 20 mmol) in dry ether (10 ml) at −78 °C under N_2. In a separate flask, to a solution of 2-(2-bromophenyl)-1,1,1-trifluoro-2-propanol (3.55 g, 20 mmol) in dry ether (10 ml) was added *n*-BuLi in hexane (1.6 M, 28 ml, 44 mmol) at −78 °C under N_2. The mixture was subsequently allowed to warm to r.t., and stirred for 14 h. The suspension formed gave a clear yellow solution upon addition of THF (10 ml). This solution was added dropwise to the former mixture at −78 °C under N_2, and the resulting solution was allowed to warm to r.t. After stirring for 4 h, the mixture was quenched with 2 M HCl, and 6 M HCl was added until the solution became acidic. The aqueous layer was extracted with ether (50 ml × 4), the combined organic layer was washed with H_2O (10 ml) and brine (20 ml), followed by drying over $MgSO_4$ and filtration. The organic solvent was then evaporated in vacuo. Purification of the residue by column chromatography (silica gel, hexane–CH_2Cl_2 = 2/1) gave hydrophosphorane **1** as a diastereomeric mixture. Combined yield, 5.42 g (57%, diastereomeric ratio = 60: 40 (**exo**:**endo**)).

1-exo: m.p. 110–111 °C; ^{1}H-NMR ($CDCl_3$) δ 1.77 (s, 3H), 7.56–7.58 (m, 2H), 7.61–7.76 (m, 4H), 8.23–8.34 (m, 2H), 8.35 (d, J_{P-H} = 712 Hz, 1H); ^{19}F-NMR ($CDCl_3$ δ −79.6 (s, 3F), −76.4 (q, J = 9.3 Hz, 3F), −75.2 (q, J = 9.3 Hz, 3F); ^{31}P-NMR ($CDCl_3$) δ −49.4; Anal. Calc. for $C_{18}H_{11}F_9O_2P$: C, 46.77; H, 2.62. Found: C, 46.47; H, 2.58%.

1-endo: m.p. 127–128 °C; ^{1}H-NMR ($CDCl_3$) δ 1.85 (s, 3H), 7.54–7.60 (m, 2H), 7.64–7.77 (m, 4H), 8.21 (dd, J = 7.3 Hz, J = 11.7 Hz, 1H), 8.29 (dd, J = 7.3 Hz, J = 10.7 Hz, 1H), 8.36 (d, J_{P-H} = 725 Hz, 1H); ^{19}F-NMR ($CDCl_3$) δ −80.8 (s, 3F), −76.3 (q, J = 9.3 Hz, 3F), −75.0 (q, J = 9.3 Hz, 3F); ^{31}P-NMR ($CDCl_3$) δ −47.8; Anal. Calc. for $C_{18}H_{11}F_9O_2P$: C, 46.77; H, 2.62. Found: C, 46.78; H, 2.42%.

*4.3. 1-Methoxy-3-methyl-3,3′,3′-tris(trifluoromethyl)-1λ^5-1,1′(3H,3′H)-spirobi(2,1-benzoxaphosphole) (**4**)*

To a solution of **1** (470 mg, 1.02 mmol, 66:34) in dry ether (5 ml) was added DBU (0.22 ml, 1.4 mmol) at r.t. After stirring for 1 h, sulfuryl chloride (0.17 ml, 2.0 mmol) was added at 0 °C, followed by addition of any excess amount of methanol (3 ml). The solution was quenched with H_2O and extracted with ether (10 ml × 3). The combined organic layer was washed with H_2O and brine, dried over $MgSO_4$ and filtered. Then, the organic solvent was evaporated in vacuo. The residue was purified by chromatography (silica gel, hexane) to give the product along with recovered material **1** (30%). Combined yield, 216 mg (44%, diastereomeric ratio = 65:35 (**exo**:**endo**)).

4-exo: m.p. 128–130 °C; ^{1}H-NMR ($CDCl_3$) δ 1.82 (s, 3H), 3.55 (d, J_{P-H} = 14.6 Hz, 3H), 7.49–7.74 (m, 6H), 8.29–8.43 (m, 2H); ^{19}F-NMR ($CDCl_3$) δ −79.9 (s, 3F), −75.2 (q, J = 9.8 Hz, 3F), −75.0 (q, J = 9.8 Hz, 3F); ^{31}P-NMR ($CDCl_3$) δ −16.1; Anal. Calc. for $C_{19}H_{14}F_9O_3P$: C, 46.36; H, 2.87. Found: C, 46.42; H, 2.88%.

4-endo: m.p. 125–127 °C; ^{1}H-NMR ($CDCl_3$) δ 1.82 (s, 3H), 3.60 (d, J_{P-H} = 14.6 Hz, 3H), 7.52–7.74 (m, 6H), 8.31–8.42 (m, 2H); ^{19}F-NMR ($CDCl_3$) δ −79.4 (s, 3F), −75.1 (s, 6F); ^{31}P-NMR ($CDCl_3$) δ −18.1; Anal. Calc. for $C_{19}H_{14}F_9O_3P$: C, 46.36; H, 2.87. Found: C, 46.51; H, 2.85%.

*4.4. 1-(1-Oxoethyl)-3-methyl-3,3′,3′-tris(trifluoromethyl)-1λ^5-1,1′(3H,3′H)-spirobi(2,1-benzoxaphosphole) (**5**)*

To solution of **1** (415 mg, 0.90 mmol, 66:34) in ether (5 ml) was added DBU (0.17 ml, 1.2 equivalents) at r.t. After stirring for 2 h, the solution was allowed to cool to 0 °C and acetyl chloride (0.1 ml, 1.3 equivalents) was added, then the mixture was stirred for 10 h at r.t. The resulting solution was quenched with sat. NH_4Cl and followed by extraction with ether (10 ml × 3). The collected organic layer was washed with brine (5 ml), dried over $MgSO_4$, filtered, and concentrated in vacuo. The crude product **5** was obtained along with starting reactant **1** (about 25% recovered). This diastereomer was separated and purified by column chromatography and TLC (silica gel, hexane–CH_2Cl_2 = 2/1). Both were recrystallized from MeCN. Combined yield, 268 mg (58%, diastereomeric ratio = 60:40 (**exo**:**endo**)).

5-exo: m.p. 147–148 °C; ^{1}H-NMR ($CDCl_3$) δ 1.67 (s, 3H), 2.21 (d, J_{P-H} = 6.3 Hz, 3H), 7.44–7.78 (m, 6H), 8.23–8.44 (m, 2H); ^{19}F-NMR ($CDCl_3$).δ −79.6 (s, 3F), −75.5 (q, J = 9.8 Hz, 3F), −74.8 (q, J = 9.8 Hz, 3F); ^{31}P-NMR ($CDCl_3$).δ −37.3; Anal. Calc. for $C_{20}H_{14}F_9O_3P$: C, 47.64; H, 2.80. Found: C, 47.49; H, 2.89%.

5-endo: m.p. 145–148 °C; ^{1}H-NMR ($CDCl_3$) δ 1.85 (s, 3H), 2.27 (d, J_{P-H} = 5.9 Hz, 3H), 7.54–7.76 (m, 6H), 8.32–8.44 (m, 2H); ^{19}F-NMR ($CDCl_3$) δ −80.6 (s, 3F), −75.8 (q, J = 9.8 Hz, 3F), −74.8 (q, J = 9.8 Hz, 3F); ^{31}P-NMR ($CDCl_3$) δ −39.1; Anal. Calc. for $C_{20}H_{14}F_9O_3P$: C, 47.64; H, 2.80. Found: C, 47.61; H, 2.81%.

4.5. 1-(1-Oxoethyl)-3,3,3′,3′-tetrakis(trifluoromethyl)-1λ⁵-1,1′(3H,3′H)-spirobi(2,1-benzoxaphosphole) (5′)

To solution of $(ML)_2PH$ (ML = the Martin ligand) (104 mg, 0.201 mmol) in ether (2 ml) was added DBU (0.04 ml, 1.2 equivalents) at r.t. After stirring for 10 min, the solution was allowed to cool to 0 °C and acetyl chloride (0.02 ml, 1.3 equivalents) was added, and then the mixture was stirred for 5 h at r.t. The resulting solution was quenched with H_2O and then extracted with ether (25 ml × 2). The collected organic layer was washed with brine (30 ml), dried over $MgSO_4$, filtered, and concentrated in vacuo. The crude product was separated by TLC (silica gel, hexane–CH_2Cl_2 = 2/1) to afford 103 mg of **5′** (92%) as a white solid. Recrystallization from MeCN yielded colorless crystals of **5′**.

5′: m.p. 164–166 °C; ^{1}H-NMR ($CDCl_3$) δ 2.26 (d, J_{P-H} = 6.0 Hz, 3H), 7.70–7.75 (m, 6H), 8.43 (dd, J = 11.4, 6.5 Hz, 2H); ^{19}F-NMR ($CDCl_3$) δ −74.9 (q, J = 9.2 Hz, 6F), −75.7 (q, J = 9.2 Hz, 6F); ^{31}P-NMR ($CDCl_3$) δ −37.1; Anal. Calc. for $C_{20}H_{11}F_{12}O_3P$: C, 43.03; H, 1.99. Found: C, 42.95; H, 1.96%.

4.6. 3-Methyl-1-methylthio-3,3′,3′-tris(trifluoromethyl)-1λ⁵-1,1′(3H,3′H)-spirobi(2,1-benzoxaphosphole) (6)

To a solution of **1** (456 mg, 0.98 mmol, 24:76) in THF (15 ml) was added DBU (0.18 ml, 1.2 mmol) at r.t. After stirring for 2 h, elemental sulfur (44 mg, 1.4 mmol) in THF was added and the mixture was stirred for 16 h to give an orange suspension. Methyl iodide (0.3 ml, 4.8 mmol) was then added. After stirring for 1 h, the solution was quenched with H_2O, followed by extraction with ether (10 ml × 3). The organic layer was dried over $MgSO_4$, filtered and concentrated in vacuo to give a crude product (diastereomeric ratio = 27:73). Diastereomeric separation and purification were achieved by TLC (silica gel, hexane–ether = 5/1) and both were recrystallized from MeCN. Combined yield, 431 mg (86%, diastereomeric ratio = 24:76 (**exo**:**endo**)).

6-exo: m.p. 136–137 °C; ^{1}H-NMR ($CDCl_3$) δ 1.82 (s, 3H), 2.21 (d, J_{P-H} = 18.1 Hz, 3H), 7.50–7.71 (m, 6H), 8.20–8.37 (m, 2H); ^{19}F-NMR ($CDCl_3$) δ −79.2 (s, 3F), −74.4 (q, J = 8.6 Hz, 3F), −74.3 (q, J = 8.6 Hz, 3F); ^{31}P-NMR ($CDCl_3$) δ −24.1; Anal. Calc. for $C_{19}H_{14}F_9O_2PS$: C, 44.89; H, 2.77. Found: C, 44.95; H, 2.55%.

6-endo: m.p. 123–124 °C; ^{1}H-NMR ($CDCl_3$) δ 1.82 (s, 3H), 2.24 (d, J_{P-H} = 18.6 Hz, 3H), 7.48–7.71 (m, 6H), 8.28–8.35 (m, 2H); ^{19}F-NMR ($CDCl_3$) δ −78.9 (s, 3F), −74.0 (s, 6F); ^{31}P-NMR ($CDCl_3$) δ −24.8; Anal. Calc. for $C_{19}H_{14}F_9O_2PS$: C, 44.89; H, 2.77. Found: C, 44.76; H, 2.60%.

4.7. 1-(Dimethylamino)-3-methyl-3,3′,3′-tris(trifluoromethyl)-1λ⁵-1,1′(3H,3′H)-spirobi(2,1-benzoxaphosphole) (7)

To a solution of **1** (290 mg, 0.63 mmol, 55:45) in THF (3 ml) was added *t*-BuLi in pentane (1.7 M, 0.42 ml, 1.1 equivalents) at −80 °C under N_2 and the resulting solution was allowed to warm to 0 °C. SO_2Cl_2 (0.08 ml, 1.5 equivalents) was then added and the reaction mixture was stirred for 0.5 h at r.t. Dimethylamine (b.p. 7 °C) which was generated from aqueous solution of dimethylamine (40% w/w) and NaOH, and passed through a KOH column was then bubbled into the solution at 0 °C. The solution was quenched with 1 M HCl and extracted with ether (50 ml × 3). The resulting organic layer was dried over $MgSO_4$, filtered and concentrated in vacuo. The diastereomers were separated and purified by TLC (silica gel, hexane–CH_2Cl_2 = 5/1) to give compound **7** along with hydroxy phosphorane (X = OH) in 38% and starting reactant **1** in 5%. The obtained product **7** was recrystallized from MeCN to yield colorless crystals. Combined yield, 103 mg (47%, diastereomeric ratio = 95:5 (**exo**:**endo**)).

7-exo: m.p. 140–141 °C; ^{1}H-NMR ($CDCl_3$) δ 1.77 (s, 3H), 2.65 (d, J_{P-H} = 11 Hz, 6H), 7.52–7.77 (m, 6H), 8.2–8.5 (m, 2H); ^{19}F-NMR ($CDCl_3$) δ −79.5 (s, 3F), −75.4 (q, J = 8.8 Hz, 3F), −75.2 (q, J = 8.8 Hz, 3F); ^{31}P-NMR ($CDCl_3$) δ −29.5; Anal. Calc. for $C_{20}H_{17}F_9NO_2P$: C, 47.54; H, 3.39; N, 2.77. Found: C, 47.37; H, 3.06; N, 2.70%.

7-endo: m.p. 142–143 °C; ^{1}H-NMR ($CDCl_3$) δ 1.72 (s, 3H), 2.62 (d, J_{P-H} = 12 Hz, 6H), 7.50–7.75 (m, 6H), 8.2–8.4 (m, 2H); ^{19}F-NMR ($CDCl_3$) δ −80.3 (s, 3F), −75.4 (q, J = 9.8 Hz, 3F), −75.2 (q, J = 9.8 Hz, 3F); ^{31}P-NMR ($CDCl_3$) δ −28.3; Anal. Calc. for $C_{20}H_{17}F_9NO_2P$: C, 47.54; H, 2.77. Found: C, 47.45; H, 2.78%.

4.8. 1-(Dimethylamino)-3,3,3′,3′-tetrakis(trifluoromethyl)-1λ⁵-1,1′(3H,3′H)-spirobi(2,1-benzoxaphosphole) (7′)

To a solution of $(ML)_2PH$ (ML = the Martin ligand) (110 mg, 0.213 mmol) in THF (2.5 ml) was added PhLi in cyclohexane–ether (1.0 M, 0.23 ml, 1.1 equivalents) at −78 °C under Ar and the resulting solution was allowed to warm to 0 °C. SO_2Cl_2 (0.03 ml, 1.8 equivalents) was then added and the reaction mixture was stirred for 20 min at 0 C. The volatile materials were removed in vacuo, and the residue was dissolved into THF (2 ml) after purging Ar. An excess amount of dimethylamine (2.0 M solution in THF, 3 ml) was added to the solution at r.t., then the solution was stirred overnight. The solution was quenched with 1 M HCl and extracted with ether (30 ml × 2). The resulting organic layer was dried over $MgSO_4$, filtered and con-

centrated in vacuo. The residue was purified by TLC (silica gel, hexane) to give 44.3 mg of compound **7′** (37%). The obtained product **7′** was recrystallized from MeCN to yield colorless crystals.

7′: m.p. 136–137 °C; ^{1}H-NMR ($CDCl_3$) δ 2.65 (d, $J_{P-H} = 11.1$ Hz, 6H), 7.63–7.71 (m, 6H), 8.39–8.44 (m, 2H); ^{19}F-NMR ($CDCl_3$) δ −75.4 (br s, 12F); ^{31}P-NMR ($CDCl_3$) δ −25.1; Anal. Calc. for $C_{20}H_{14}F_{12}NO_2P$: C, 42.95; H, 2.52; N, 2.50. Found: C, 42.90; H, 2.50; N, 2.40%.

4.9. 1,3-Dimethyl-3,3′,3′-tris(trifluoromethyl)-1λ^5-1,1′(3H,3′H)-spirobi(2,1-benzoxaphosphole) (**8**)

To a solution of **1** (48 mg, 0.1 mmol, 20:80) in THF (3 ml) was added DBU (1.8-diazabicycle[5.4.0]undec-7-ene, 0.025 ml, 0.17 mmol) at r.t. After stirring for 2 h, excess methyl iodide (0.2 ml, ca. 30 mmol) was added. The solution was quenched with H_2O, followed by extraction with ether (10 ml × 3). The resulting organic layer was dried over $MgSO_4$ and filtered. The organic solvent was evaporated in vacuo. The residue was recrystallized from MeCN to give **8**. The diastereomers could not be separated by TLC. However, they could be separately prepared from their corresponding diastereomerically pure **1**. Combined yield, 31 mg (62%, diastereomeric ratio = 19:81 (**exo**:**endo**)).

8-exo: m.p. 116–117 °C; ^{1}H-NMR ($CDCl_3$) δ 1.75 (s, 3H), 2.03 (d, $J_{P-H} = 16.6$ Hz, 3H), 7.50–7.58 (m, 2H), 7.60–7.71 (m, 4H), 8.33 (dd, $J = 7.8$ Hz, $J = 11.1$ Hz, 1H), 8.39 (m, 1H); ^{19}F-NMR ($CDCl_3$) δ −79.8 (s, 3F), −75.5 (q, $J = 9.8$ Hz, 3F), −75.3 (q, $J = 9.8$ Hz, 3F); ^{31}P-NMR ($CDCl_3$) δ −26.9; Anal. Calc. for $C_{19}H_{14}F_9O_2P$: C, 47.92; H, 2.96. Found: C, 48.04; H, 2.64%.

8-endo: m.p. 118–120 °C; ^{1}H-NMR ($CDCl_3$) δ 1.75 (s, 3H), 2.11 (d, $J_{P-H} = 16.7$ Hz, 3H), 7.48–7.58 (m, 2H), 7.60–7.72 (m, 4H), 8.31 (dd, $J = 7.8$ Hz, $J = 11.2$ Hz, 1H), 8.40 (m, 1H); ^{19}F-NMR ($CDCl_3$) δ −80.1 (s, 3F), −75.4 (q, $J = 9.8$ Hz, 3F), −74.9 (q, $J = 9.8$ Hz, 3F); ^{31}P-NMR ($CDCl_3$) δ −26.1; Anal. Calc. for $C_{19}H_{14}F_9O_2P$: C, 47.92; H, 2.96. Found: C, 47.94; H, 2.61%.

4.10. 1-Butyl-3-methyl-3,3′,3′-tris(trifluoromethyl)-1λ^5-1,1′(3H,3′H)-spirobi(2,1-benzoxaphosphole) (**9**)

To a solution of **1** (119 mg, 0.29 mmol, exo:endo = $< 2: > 98$) in ether (3 ml) was added DBU (1.8-diazabicycle[5.4.0]-undec-7-ene, 0.05 ml, 0.32 mmol) at r.t. After stirring for 2 h, *n*-butyl bromide (0.06 ml, 0.58 mmol) was added. The solution was quenched with H_2O, followed by extraction with ether (10 ml × 3). The resulting organic layer was dried over $MgSO_4$ and filtered. The organic solvent was evaporated in vacuo. PTLC (hexane–CH_2Cl_2 = 5/1, silica gel) was performed yielding **9-endo** (colorless oil 63%). The same procedure was carried out for **1-exo** to prepare the other diastereomer **9-exo** (63%). Combined yield, 83 mg (63%, diastereomeric ratio = $< 2: > 98$ (**exo**:**endo**)).

9-exo: ^{1}H-NMR ($CDCl_3$) δ 0.82 (t, $J = 7.3$ Hz, 3H), 1.28 (m, 2H), 1.57–1.83 (m, 2H), 1.76 (s, 3H), 2.21 (dt, $J_{P-H} = 15$ Hz, $J = 7.3$ Hz, 2H), 7.51–7.72 (m, 6H), 8.34–8.43 (m, 2H); ^{19}F-NMR ($CDCl_3$) δ −79.67 (s, 3F), −75.4 (m, 6F); ^{31}P-NMR ($CDCl_3$) δ −22.2; HRMS (FAB^+) Calc. for $C_{22}H_{20}F_9O_2P$: 519.1141. Found: 519.1125.

9-endo: ^{1}H-NMR ($CDCl_3$) δ 0.81 (t, $J = 7.3$ Hz, 3H), 1.26 (m, 2H), 1.68–1.84 (m, 2H), 1.73 (s, 3H), 2.22 (dddd, $J_{P-H} = 12$ Hz, $^2J = 12$ Hz, $^3J = 12$ Hz, $^3J = 4$ Hz, 1H), 2.41 (dddd, $J_{P-H} = 17$ Hz, $^2J = 12$ Hz, $^3J = 12$ Hz, $^3J = 5$ Hz, 1H), 7.44–7.80 (m, 6H), 8.26–8.45 (m, 2H); ^{19}F-NMR ($CDCl_3$) δ −80.1 (s, 3F), −75.4 (q, $J = 9.7$ Hz, 3F), −75.0 (q, $J = 9.7$ Hz, 3F); ^{31}P-NMR ($CDCl_3$) δ −22.6; Anal. Calc. for $C_{22}H_{20}F_9O_2P$: C, 50.98; H, 3.89. Found: C, 50.77; H, 3.90%.

4.11. Kinetic measurements

Freshly distilled toluene, *p*-xylene or 4-butyltoluene was used as solvent and the diastereomerically enriched samples were sealed in NMR tubes under N_2. Kinetic measurements of pseudorotation processes were carried out with a JEOL EX-400 spectrometer by monitoring the diastereomeric ratio from the integration of ^{19}F-NMR signals. The range of temperature of the rate measurements were 40–70 °C for **1**, 40–70 °C for **4**, 90–125 °C for **5**, 85–110 °C for **6**, 130–170 °C for **7**, 150–180 °C for **8**, and 160–185 °C for **9**.

The data was analyzed based upon reversible first-order kinetics using the equation of

$$\ln[(x_e - x_0)/(x_e - x)] = k_-(K+1)t$$

where x_e is the equilibrium ratio, x_0 is the ratio observed at $t = 0$, x is the ratio observed at constant intervals, k_- is the rate constant (**endo** to **exo**), and K is the equilibrium constant ($K = (100 - x_e)/x_e = k_+/k_-$). Least square analyses provided the rate constants given in Table 2. The activation parameters were calculated from the Eyring plot of the rates at four different temperatures or more.

4.12. X-ray structure determinations

For **1-exo**, measurements were carried out on a Mac Science MXC3 diffractometer with graphite-monochromated Mo–K_α radiation ($\lambda = 0.71073$ Å) for data collection. Lattice parameters were determined by least-square fitting of 31 reflections with $51 < 2\theta < 60°$. Data were collected with the $2\theta/\omega$ scan mode. All data were corrected for extinction. The structures were solved by a direct method with the SIR-92 program [16].

The hydrogen atoms were included in the refinement on geometrically calculated positions (C–H = 1.0 Å) riding on their carrier atoms with isotropic thermal parameters. For **5′** and **7′**, measurements were carried out on a Mac Science DIP2030 imaging plate instrument equipped with graphite-monochromated Mo–K_α radiation ($\lambda = 0.71073$ Å). Unit cell parameters were determined by autoindexing several images in each data set separately with the DENZO program [17]. For each data set, rotation images were collected in 3° increments with a total rotation of 180° about ϕ. Data were processed by using the SCALEPACK program [17]. The structures were solved by a direct method and refined by full-matrix least-squares methods with the TeXsan program [16]. All non-hydrogen atoms were refined with anisotropic thermal parameters and were included in the refinement at calculated positions (C–H = 1.0 Å) riding on their carrier atom with isotropic thermal parameters. The structures were solved by a direct method with the SIR-92 program.

5. Supplementary material

Crystallographic data (excluding structure factors) for the structures reported in this paper have been deposited with the Cambridge Crystallographic Data Center, CCDC nos. 168164 (**5′**), 168165 (**7′**), and 168166 (**1-exo**). Copies of this information may be obtained free of charge from The Director, CCDC, 12 Union Road, Cambridge CB2 1EZ, UK (Fax: +44-1223-336033; e-mail: deposit@ccdc.cam.ac.uk or www: http://www.ccdc.cam.ac.uk).

References

[1] (a) F.H. Westheimer, Acc. Chem. Res. 1 (1968) 70;
(b) G.R.J. Thatcher, R. Kluger, Adv. Phys. Org. Chem. 25 (1989) 99 and references cited therein.

[2] R.R. Holmes, Pentacoordinated Phosphorus—Structure and Spectroscopy, Vols. I, II, ACS Monograph 175, 176, American Chemical Society, Washington, DC, 1980.

[3] R.S. Berry, J. Chem. Phys. 32 (1960) 933.

[4] E.L. Muetterties, W. Mahler, R. Schmutzler, Inorg. Chem. 2 (1963) 613.

[5] J. Moc, K. Morokuma, J. Am. Chem. Soc. 117 (1995) 11790 and references therein.

[6] (a) S. Trippett, Phosphorus Sulfur 1 (1976) 89;
(b) S. Trippett, Pure Appl. Chem. 40 (1970) 595;
(c) G. Buono, J.R. Llinas, J. Am. Chem. Soc. 103 (1981) 4532;
(d) M. Eisenhut, H.L. Mitchell, D.D. Traficante, R.J. Kaufman, J.M. Deutch, G.M. Whitesides, J. Am. Chem. Soc. 96 (1974) 5385;
(e) C.G. Moreland, G.O. Doak, L.B. Littlefield, N.S. Walker, J.W. Gilje, R.W. Braun, A.H. Cowley, J. Am. Chem. Soc. 98 (1976) 2161;
(f) L.V. Griend, R.G. Cavell, Inorg. Chem. 22 (1983) 1817.

[7] (a) R. Hoffmann, J.M. Howell, E.L. Muetterties, J. Am. Chem. Soc. 94 (1972) 3047;
(b) R.S. McDowell, A. Streitwieser Jr., J. Am. Chem. Soc. 107 (1985) 5849;
(c) J.A. Deiters, R.R. Holmes, J.M. Holmes, J. Am. Chem. Soc. 110 (1988) 7672;
(d) P. Wang, Y. Zhang, R. Glaser, A.E. Reed, P.v.R. Schleyer, A. Streitwieser, J. Am. Chem. Soc. 113 (1991) 55;
(e) H. Wasada, K. Hirao, J. Am. Chem. Soc. 114 (1992) 16;
(f) G.R.J. Thatcher, A.S. Campbell, J. Org. Chem. 58 (1993) 2272;
(g) P. Wang, Y. Zhang, R. Glaser, A. Streitwieser, P.v.R. Schleyer, J. Comput. Chem. 14 (1993) 522;
(h) G.R.J. Thatcher, E.S. Krol, D.R. Cameron, J. Chem. Soc. Perkin Trans 2 (1994) 683;
(i) B.D. Wladkowski, M. Krauss, W.J. Stevens, J. Phys. Chem. 99 (1995) 4490.

[8] (a) W.H. Stevenson III, S. Wilson, J.C. Martin, W.B. Farnham, J. Am. Chem. Soc. 107 (1985) 6340;
(b) I. Granoth, J.C. Martin, J. Am. Chem. Soc. 101 (1979) 4618 and 4623;
(c) E.F. Perozzi, R.S. Michalak, G.D. Figuly, W.H. Stevenson III, D.B. Dess, M.R. Ross, J.C. Martin, J. Org. Chem. 46 (1981) 1049;
(d) M.R. Ross, J.C. Martin, J. Am. Chem. Soc. 103 (1981) 1234;
(e) J.C. Martin, Science 221 (1983) 509;
(f) S.K. Chopra, J.C. Martin, Heteroatom Chem. 2 (1991) 71;
(g) C.D. Moon, S.K. Chopra, J.C. Martin, in: E.N. Walsh, E.J. Griffiths, R.W. Parry, L.D. Quin (Eds.), Phosphorus Chemistry, Developments in American Science, ACS Symposium Series 486, American Chemical Society: Washington, DC, 1992, pp. 128–136.

[9] (a) S. Kojima, K. Kajiyama, K.-y. Akiba, Tetrahedron Lett. 35 (1994) 7037;
(b) S. Kojima, K. Kajiyama, K.-y. Akiba, Bull. Chem. Soc. Jpn. 68 (1995) 1785;
(c) K. Kajiyama, S. Kojima, K.-y. Akiba, Tetrahedron Lett. 37 (1996) 8409;
(d) S. Kojima, K. Kajiyama, M. Nakamoto, K.-y. Akiba, J. Am. Chem. Soc. 118 (1996) 12866;
(e) K. Kajiyama, M. Yoshimune, M. Nakamoto, S. Matsukawa, S. Kojima, Y. Yamamoto, K.-y. Akiba, Org. Lett. 4 (2001) 1873.

[10] Preliminary results have been reported in part in the following: (a) S. Kojima, M. Nakamoto, K. Kajiyama, K.-y. Akiba, Tetrahedron Lett. 36 (1995) 2261; (b) S. Kojima, M. Nakamoto, K. Yamazaki, K.-y. Akiba, Tetrahedron Lett. 38 (1997) 4107.

[11] (a) For the systematic examination of the pseudorotation of pentacoordinate silicates using Martin ligands: [8a];
(b) For pentacoordinate stiboranes: S. Kojima, Y. Doi, M. Okuda, K.-y. Akiba, Organometallics 14 (1995) 1928.

[12] K. Mislow, Acc. Chem. Res. 3 (1970) 321.

[13] (a) J.E. Huheey, J. Phys. Chem. 69 (1965) 3284;
(b) J.E. Huheey, J. Phys. Chem. 70 (1966) 2086.

[14] P.R. Wells, Prog. Phys. Org. Chem. 6 (1968) 111.

[15] M. Charton, Prog. Phys. Org. Chem. 13 (1981) 119.

[16] TeXsan: Single-Crystal Analysis Software, version 1.9; Molecular Structure Corporation: The Woodlands, TX 77381, USA, 1998. The program is available from Mac Science Co.

[17] Z. Otwinowsky, W. Minor, DENZO and SCALEPACK. in: C.W. Carter, Jr., R.M. Sweet (Eds.), Processing of X-ray Diffraction Data Collected in Oscillation Mode, Methods in Enzymology, Vol. 276, Macromolecular Crystallography, Part A; Academic Press: New York, 1997, pp. 307–326. The program is available from Mac Science Co.